Calculating Radiated Emissions Due to I/O Line Coupling on Printed Circuit Boards Using the Imbalance Difference Method

Changyi Su, *Student Member, IEEE*, and Todd H. Hubing, *Fellow, IEEE*

***Abstract*—High frequency signals on printed circuit board (PCB) traces can couple to I/O nets that carry the coupled energy away from the board resulting in significant radiated emissions. Automated tools to detect unacceptable levels of coupling during the board layout rely on fast methods for estimating the amount of coupling and the resulting radiated emissions. A modeling technique is proposed to speed up the analysis of PCBs with coupled traces that induce common-mode currents on attached cables. Based on the concept of imbalance difference, differential-mode sources are converted to equivalent common-mode sources that drive the attached cable and the PCB reference plane. A closed-form expression based on the imbalance difference model is developed to estimate the maximum radiated emissions due to I/O line coupling in PCBs.**

***Index Terms*—Common mode, electromagnetic modeling, electromagnetic radiation, imbalance difference model.**

I. Introduction

CROSSTALK is a significant concern for printed circuit board (PCB) designers. Coupling between signal lines can cause electromagnetic interference as well as signal integrity problems. Crosstalk between signal traces and traces that connect to wires that bring signals or power onto the board (I/O lines) can be particularly troublesome. Although crosstalk can be minimized by careful routing of signal and I/O traces, there is always some amount of crosstalk in practical designs. Automated tools to detect unacceptable levels of coupling during the board layout rely on methods for estimating the amount of coupling and the resulting radiated emissions. Calculating levels of crosstalk is particularly challenging when one of the traces is an I/O trace, because the termination impedance of the trace may be unknown.

One approach for analyzing the radiated emissions due to coupling between signal and I/O lines in a PCB is to simulate the interconnect system using a 3-D full-wave electromagnetic modeling simulator. Full-wave models can provide accurate solutions to well-defined problems, but they require significant computational resources and they cannot predict how small changes in the structure will affect the results without repeated analysis with changes explicitly implemented. For these reasons, full-wave models are not a practical option for providing fast estimates of worst case radiated emissions during the initial design and routing processes.

Extensive research has been devoted to develop fast and accurate techniques for crosstalk analysis [1]–[6], the first component of this problem. Less research has been done on the antenna model and the radiated emission estimation, but simple equations were derived by assuming that the attached cable was an isotropic radiator in [7]. In [8], the attached cable is a parallel wire transmission line with known characteristic impedance. Radiated emissions from the transmission line are determined by full-wave modeling. Maximum radiated field estimates based on dipole antenna models were presented in [9]–[12]. In these models, a common-mode voltage source was applied between the cable and the PCB reference plane at the connector; but the input impedance of the antenna was required in order to determine the magnitude of this common-mode voltage. In these previous papers, either simulations [9], [10] or measurements [11] were used to obtain the impedance of the antenna. In [7] and [12], a worst case estimate of the antenna impedance, based on a resonant half-wave dipole, was used. This method does not require simulation or measurement of the input impedance of the antenna and provides a reasonable estimate of the worst case radiated emissions. However, it cannot account for the interaction between the reactive parts of the antenna and circuit impedances.

In Section II, a Thevenin equivalent source model for the coupling to the I/O trace is derived. This source model accounts for all of the coupling without requiring the input impedance of the attached cable to be known in advance. Section III introduces a model for calculating the radiated emissions due to I/O coupling on PCBs that significantly reduces simulation times without sacrificing the accuracy of the results. The model is derived based on the concept of imbalance difference [13]–[17]. The differential-mode signals on the signal traces are converted to equivalent common-mode sources quantitatively using a parameter called the *imbalance factor*. In the imbalance difference model, the lines carrying differential signals on the PCB are replaced by equivalent common-mode sources. This model separates the radiation problem from the PCB coupling problem and provides a fast method for calculating the radiated fields from the PCB due to coupling between signal and I/O lines. In Section IV, a closed-form expression is developed based on the imbalance difference model to predict the maximum radiated

Manuscript received May 29, 2011; revised July 27, 2011; accepted September 7, 2011. Date of publication October 13, 2011; date of current version February 17, 2012. This work was supported in part by the NSF Industry/University Cooperative Research Center for Electromagnetic Compatibility.

The authors are with Clemson University, Clemson, SC 29634 USA (e-mail: csu@clemson.edu; hubing@clemson.edu).

Color versions of one or more of the figures in this paper are available online at http://ieeexplore.ieee.org.

Digital Object Identifier 10.1109/TEMC.2011.2168565

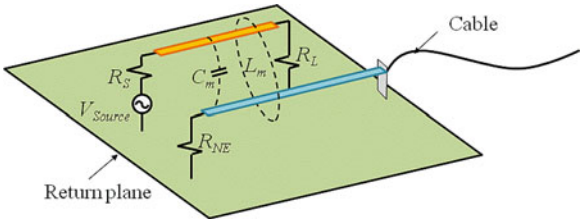

Fig. 1. Schematic representation of signal coupling to an I/O line.

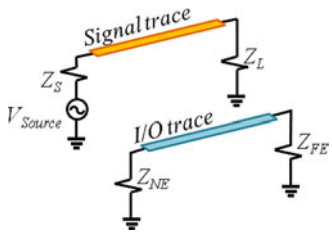

Fig. 2. Equivalent circuit illustrating crosstalk.

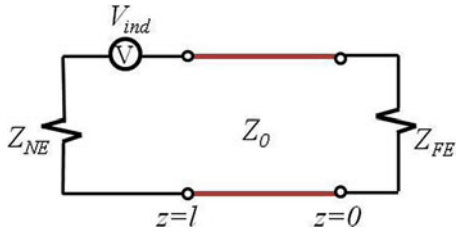

Fig. 3. Magnetic coupling model of the victim circuit.

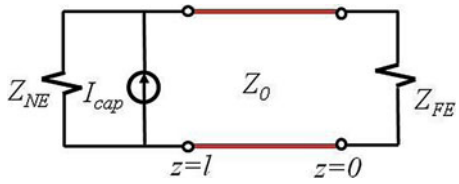

Fig. 4. Capacitive coupling model of the victim circuit.

emissions from the structure. The accuracy of the model and the closed-form expression are evaluated in Section V.

II. Thevenin Equivalent Coupling Source

A schematic illustrating the coupling from a high-speed signal trace to an adjacent I/O line is shown in Fig. 1. The signal trace and the I/O line are routed next to each other over a wide ground plane. The signal trace is connected to a signal source at one end and terminated with a load at the other end. The I/O trace is terminated with a resistance at the near-end and a wire extending beyond the return plane at the far-end. Signals can be coupled to the I/O circuit by magnetic-field coupling or electric-field coupling. Magnetic-field (or inductive) coupling occurs when magnetic flux lines from the source circuit pass through the loop formed by the I/O trace circuit and the return plane. Schematically, magnetic-field coupling is represented by a mutual inductance L_m between the two loops. Similarly, a mutual capacitance C_m between the two traces is used to indicate that energy is coupled from the source circuit to the victim circuit through an electric field (i.e., capacitive coupling).

In this paper, the analysis of this problem is broken into three distinct stages.

1) Developing the equivalent lumped-element circuit model for the two coupling mechanisms and determining the total voltage coupled to the victim circuit.
2) Developing a relative simple imbalance difference model for the complex geometry.
3) Analyzing the simplified model to determine either the actual or worst case radiated emissions.

To calculate the crosstalk between the coupled lines, consider the equivalent circuit shown in Fig. 2. A source circuit consists of a source voltage V_{source} and a source impedance Z_S, which is connected to a load Z_L via a signal trace. This may represent an entire circuit or a portion of a longer circuit that couples to the I/O line. Two other terminations, denoted as Z_{NE} and Z_{FE}, are connected to the I/O trace. The circuit terminations are known and have variable values, with the exception of the far-end load of the I/O trace Z_{FE}, where the cable is attached. Z_{FE} is the input impedance of the antenna formed by the cable being driven against the circuit board return plane.

Assuming the lines are weakly coupled, the total coupling is a linear combination of contributions due to the inductive and capacitive coupling [5]. In Fig. 3, the I/O trace and return plane are represented as a transmission line of length l. One end of the transmission line is connected to a voltage source V_{ind}, which represents the induced electromotive force due to inductive coupling.

If the portion of the signal trace that couples to the I/O trace is electrically short with a self-capacitance and self-inductance that are negligible compared to the source and load impedances, the signal voltage on the trace is $V_{signal} = V_{source}(Z_L/Z_L + Z_S)$and the current is given by $I_{signal} = V_{signal}/Z_L$; the induced voltage due to inductive coupling is given by

$$V_{ind} = \frac{-j\omega L_m}{Z_L} V_{signal} \tag{1}$$

where L_m is the mutual inductance between the signal trace circuit and the I/O trace circuit.

In Fig. 4, an independent current source I_{cap} represents the induced current due to capacitive coupling.

The induced current source amplitude is

$$I_{cap} = j\omega C_m V_{signal} \tag{2}$$

where C_m is the mutual capacitance between the signal trace and the I/O trace.

The total voltage induced in the victim circuit is the linear superposition of the two equivalent coupling sources

$$\begin{aligned} V_{total} &= V_{ind} + V_{cap} \\ &= j\omega \left[\frac{-L_m}{Z_L} + C_m Z_{NE} \right] V_{signal}. \end{aligned} \tag{3}$$

Note that the derivation of (3) assumed that the signal trace (or portion of the signal trace coupling to the I/O line) was

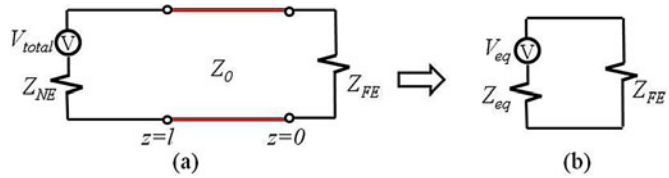

Fig. 5. Equivalent circuits for the I/O line structure. (a) Near-end equivalent circuit and transmission line. (b) Thevenin equivalent circuit at the connector.

electrically short. This is frequently the case, but similar equations that do not depend on the value of Z_{FE} could be readily derived for longer signal traces.

The I/O trace may or may not be electrically short and is modeled as a transmission line as indicated in Fig. 5(a). The open-circuit voltage at the far end (i.e., the connector) V_{eq}, and the equivalent impedance looking back toward the near end from the connector Z_{eq}, can be readily calculated from transmission line theory [18] yielding the Thevenin equivalent circuit in Fig. 5(b).

The general solution for the voltage on a lossless transmission line is

$$V(z) = V_0^+ e^{-j\beta z} + V_0^- e^{j\beta z} \tag{4}$$

where V_0^+ and V_0^- are the voltage amplitudes of the incident and reflected waves, respectively. The Thevenin voltage for the circuit in Fig. 5(a) is [5]

$$V_{eq} = 2\left(\frac{Z_0}{Z_0 + jZ_{NE}\tan\beta l}\right)\left(\frac{V_{total}}{e^{j\beta l} + e^{-j\beta l}}\right) \tag{5}$$

where Z_0 is the characteristic impedance of the transmission line and β is the wavenumber. Replacing V_{total} with (3), the magnitude of V_{eq} is

$$|V_{eq}| = \left|\frac{V_{signal}}{\cos\beta l}\right|\left|\frac{Z_0}{Z_0 + jZ_{NE}\tan\beta l}\right| \times \left|-\omega L_m \frac{1}{Z_S + Z_L} + \omega C_m \frac{Z_{NE}Z_L}{Z_S + Z_L}\right|. \tag{6}$$

The Thevenin equivalent impedance is

$$Z_{eq} = Z_0\left(\frac{Z_{NE} + jZ_0\tan\beta l}{Z_0 + jZ_{NE}\tan\beta l}\right). \tag{7}$$

For most signal and I/O trace configurations, the mutual inductance and capacitance in (6) can be calculated based on the concept of even-mode and odd-mode capacitances [19].

III. Imbalance Difference Model

In Section II, the complex geometry in Fig. 1 was simplified by removing the signal trace circuit and applying the total induced voltage source to the victim circuit, as shown in Fig. 6(a). The development of the simplified circuit in Fig. 6(a) does not require any prior knowledge of the impedance at the cable end of the I/O circuit. In this section, the structure in Fig. 6(a) is further simplified using the imbalance difference theory first proposed by Watanabe *et al*. [13] and further developed in [14]–[17]. According to this theory, the differential- to common-mode conversion occurs at points where there is a change in the imbalance.

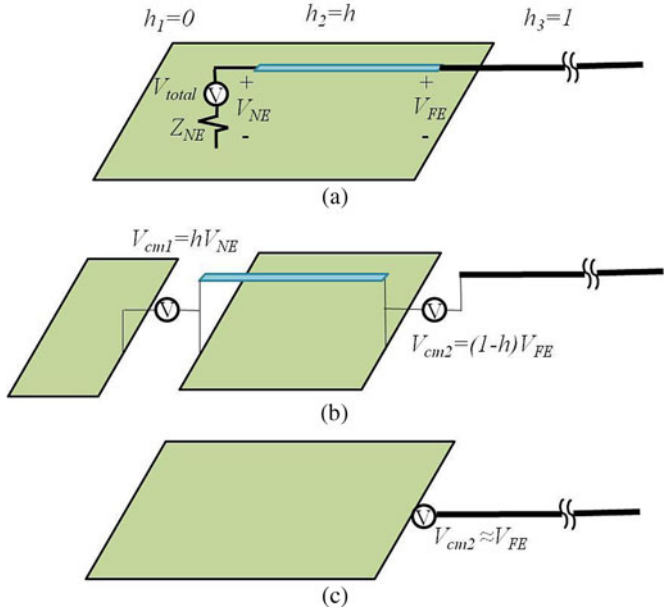

Fig. 6. Imbalance difference model for the I/O line structure. (a) Full model. (b) Imbalance difference model. (c) Simplified imbalance difference model.

In Fig. 6(a), the value of the imbalance parameter *h* changes at both ends of the microstrip. Hence, the common-mode current on the cable in Fig. 6(a) is equivalent to the current on the cable in Fig. 6(b). In Fig. 6(b), the ground plane is driven against the cable by two common-mode sources. The amplitude of each common-mode source is the product of the differential-mode voltage and the change in the imbalance factor that occurs at each end of the I/O trace. Since the width of the trace is usually much smaller than that of the board, the change in the imbalance at the source end of the trace is very close to zero. Hence, the magnitude of the first common-mode source V_{CM1} is close to zero. The change in the imbalance factor at the other end is very close to 1. Therefore, the magnitude of the second common-mode source V_{CM2} is approximately equal to the differential-mode voltage V_{FE} at the connector. With these approximations, the equivalent model in Fig. 6(b) can be further simplified to the model in Fig. 6(c) in which the board is driven by the differential-mode voltage at the load end of the I/O trace.

From the circuit in Fig. 6(c), the voltage driving the cable depends on the value of the antenna impedance. The input impedance of the dipole-type antenna in Fig. 6(c) is a complex function of frequency that can only be determined by full-wave simulation or measurement. To avoid doing this, the equivalent model in Fig. 6(c) is replaced by the Thevenin equivalent model derived in the previous section. In the new model (see Fig. 7) for cable current calculations, the simplified source in Fig. 7 is equivalent to the original circuit in Fig. 1 and does not require any assumptions about the antenna input impedance.

In this model, both the I/O line and the dielectric layer were deleted from the model. While these play an important role in the crosstalk calculation (and therefore in full-wave simulations of the entire structure), they are relatively unimportant after the amplitude of the common-mode source has been determined. Eliminating the I/O line and the dielectric layer from

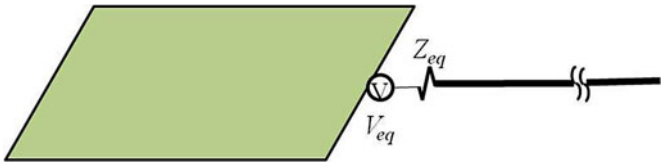

Fig. 7. Imbalance difference model.

the equivalent model significantly reduces the simulation time while still yielding good results.

IV. Maximum Radiated Emission Estimation

A full-wave analysis of the radiated emissions from the simplified model in Fig. 7 will yield virtually the same results as a full-wave analysis of the much more complex configuration in Fig. 1. However, very often for electromagnetic compatibility problem analysis, it is much more useful to obtain the maximum emissions from the PCB for all possible cable lengths and orientations than it is to obtain the emission from one specific cable geometry. A closed-form formula was developed in [20] to estimate the maximum radiated emissions from the antenna model in Fig. 7. This formula was enhanced in [21] to be more accurate over larger frequency ranges. When a board is driven by an ideal common-mode source V_{CM}, the maximum electric field can be calculated as

$$|E|_{\max} \simeq \begin{cases} 20 \times I_{peak} \times \dfrac{2}{\sin\left(\sqrt{2}\right)} & f \le \dfrac{c_0}{2l_{cable}} \\ 20 \times I_{peak} \times \dfrac{2}{\sin\left(\sqrt{\frac{c_0}{f l_{cable}}}\right)} & f > \dfrac{c_0}{2l_{cable}} \end{cases} \tag{8}$$

where l_{cable} is the length of the attached cable, f is the frequency, and c_0 is the propagation velocity in free space. I_{peak} is the highest current that actually exists on the cable and is given by

$$I_{peak} = \frac{V_{CM}}{R_{\min}} \times \text{board\_factor} \times \text{cable\_factor} \tag{9}$$

where $R_{\min}$ is the input resistance (about 37 Ω) of a resonant quarter-wave monopole. Two factors account for the effect that the finite cable length and the small board size have on this minimum resistance

$$\text{board\_factor} = \begin{cases} \sin\left(2\pi l_{board}/\lambda\right) & \text{when } l_{board} \le \frac{\lambda}{4} \\ 1.0, & \text{otherwise} \end{cases} \tag{10}$$

$$\text{cable\_factor} = \begin{cases} \sin\left(2\pi l_{cable}/\lambda\right) & \text{when } l_{cable} \le \frac{\lambda}{4} \\ 1.0, & \text{otherwise} \end{cases} \tag{11}$$

where

$$l_{board} = \frac{1 + 2L/W}{2L/W} \times \sqrt{L^2 + W^2}$$

and where L and W denote the board length and width, respectively.

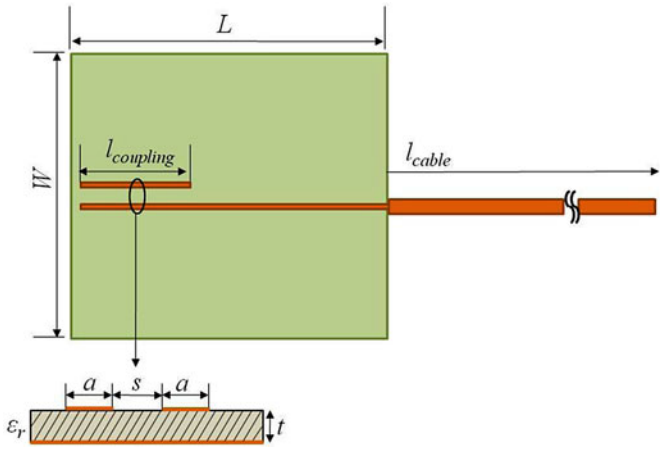

Fig. 8. Test geometry.

TABLE I
Simulation Configurations

Test Case	Geometrical parameters					Dielectric constant ε_r	L_m (nH)	C_m (pF)
	a/t	s/t	$L_{coupling}$ (mm)	L (mm)	W (mm)			
1	0.5	0.5	20	100	100	1.0	3.3	0.13
2	0.5	1.0	20	100	100	1.0	2.1	0.078
3	1.0	0.5	20	100	100	1.0	2.3	0.16
4	0.5	0.5	40	100	100	1.0	6.5	0.27
5	0.5	0.5	20	100	40	1.0	3.3	0.13
6	0.5	0.5	20	100	100	4.0	3.3	0.28

The common-mode source in Fig. 7 is connected to the equivalent impedance Z_{eq}. Since this impedance value is not affected by the cable length and source location, the highest current on the cable can be written as

$$I_{peak} = \frac{V_{eq}}{\left| Z_{eq} + \frac{R_{\min}}{\text{board\_factor} \times \text{cable\_factor}} \right|}. \tag{12}$$

For the model in Fig. 7, (8)–(12) can be used to estimate the maximum radiated electric field strength at a distance of 3 m from the board.

V. Validation

In order to validate the equivalent model in Fig. 7, the radiated fields from various I/O coupling geometries were calculated using a full-wave numerical modeling code [22]. The modeled test board and the coupled traces are shown in Fig. 8. The test board has dimensions $L \times W$. A cross-sectional view of the coupled microstrip line structure is also shown in Fig. 8. The signal trace is driven by a 1-V, 50-Ω voltage source at one end and terminated with a 50-Ω load at the other end. An I/O trace is routed parallel to the signal trace and extended beyond the edge of the board where it drops to an infinite ground plane 1 m below. The near-end of the I/O trace is terminated with a 50-Ω resistor. The space between the traces and the ground plane is filled with a dielectric material that has a dielectric constant ε_r.

Both the geometry and the dielectric constant were varied as indicated in Table I. The relevant geometric parameters include

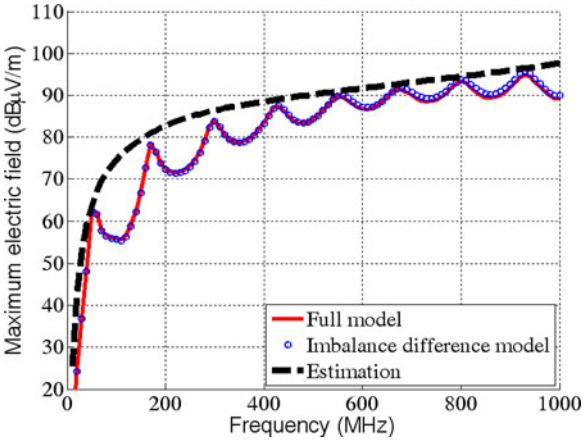

Fig. 9. Maximum radiation for Case 1.

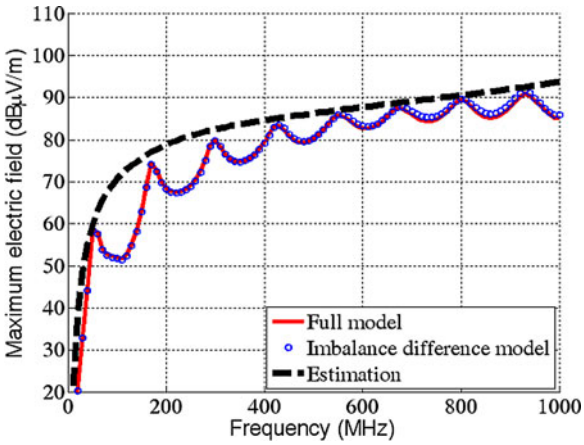

Fig. 10. Maximum radiation for Case 2.

the trace width-to-height ratio (a/t), the separation-to-height ratio (s/t), the coupling length, and the board width.

Fig. 9 shows radiated field calculated using a full-wave simulation of the entire structure (full model) and the simplified model in Fig. 7 (imbalance difference model), along with the maximum emissions estimate for Case 1. The imbalance difference model yields results that are in good agreement with the original configuration over the entire 10–1000 MHz frequency range. The closed-form expression estimates the peak emissions from the board within a few decibels at every resonant frequency. Figs. 10–13 show similar plots for test cases 2–5. In all the cases, the difference between the simulations and the estimate is within a few decibels.

In Case 6, where the dielectric constant is 4.0, the agreement between the full model (with dielectric) and the imbalance difference model (no dielectric) is still excellent as indicated in Fig. 14. This demonstrates that the presence of the dielectric is not required after the model has been simplified using the imbalance difference model. Eliminating the dielectric layer from the imbalance difference model significantly reduces the simulation time without sacrificing the accuracy of the results.

Of course, it would be unusual (though not unheard of) to have a trace connect to a solitary wire exiting the board. Additional wires, with at least one of them connected to the circuit board

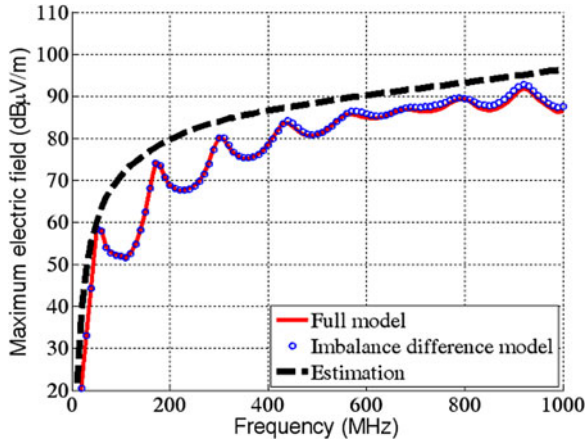

Fig. 11. Maximum radiation for Case 3.

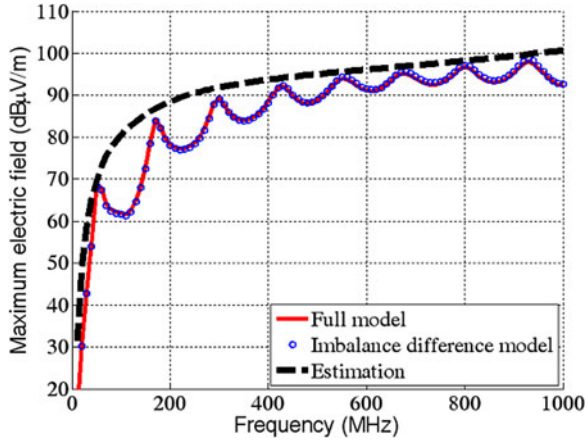

Fig. 12. Maximum radiation for Case 4.

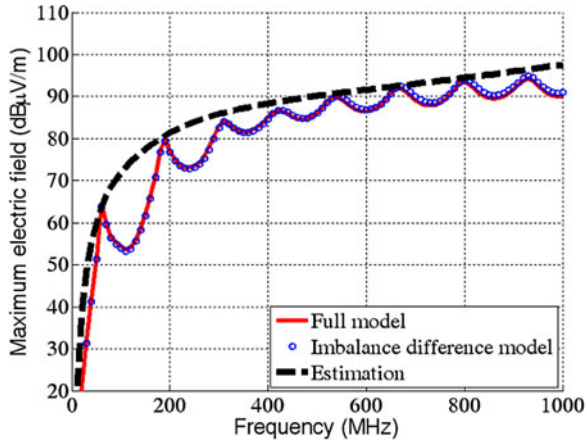

Fig. 13. Maximum radiation for Case 5.

ground, are likely to share the same connector and cable bundle. These additional wires can confound the techniques described in [9]–[12], because the termination impedance Z_{FE} is now a function of both the differential and common-mode impedances of the cable. However, the model in Fig. 7 is not affected by the presence of these additional wires. It depends only on sources and structures located on the board. Additional wires or ground

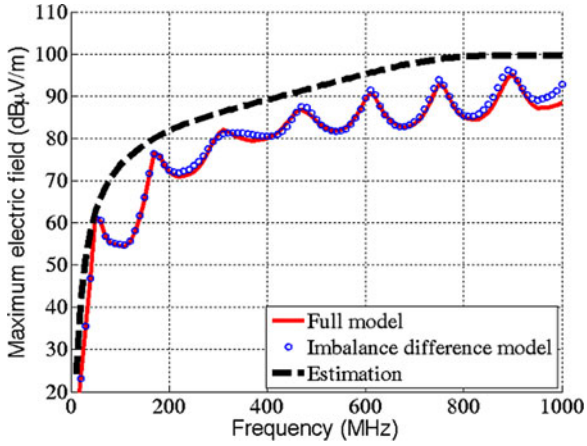

Fig. 14. Maximum radiation for Case 6.

extensions can be added next to the I/O wire in Fig. 7, without changing the values of V_{eq} or Z_{eq}. The imbalance difference model is well suited for determining the equivalent common-mode sources for geometries like this [14], [16].

VI. Conclusion

A modeling technique has been presented to speed up the analysis of PCBs with coupled traces that induce common-mode currents on attached cables. Based on the concept of imbalance difference, differential-mode sources are converted to equivalent common-mode sources that drive the attached cable and the PCB reference plane. The proposed model does not require simulating or estimating the antenna input impedance presented by the attached cable. In this model, the differential-mode sources and traces are replaced with a common-mode voltage source that drives the attached cable against the reference plane. The detailed structures of the traces are eliminated prior to modeling the radiated emissions, so the analysis of the equivalent model generally requires much less computational resources than an analysis of the full model.

References

[1] B. D. Jarvis, "The effects of interconnections on high-speed logic circuits," *IEEE Trans. Electron. Comput.*, vol. EC-12, no. 5, pp. 476–487, Oct. 1963.
[2] J. A. DeFalco, "Predicting crosstalk in digital systems," *Comput. Design*, vol. 12, no. 6, pp. 69–75, Jun. 1973.
[3] Y.-S. Sohn, J.-C. Lee, H.-J. Park, and S.-I. Cho, "Empirical equations on electrical parameters of coupled microstrip lines for crosstalk estimation in printed circuit board," *IEEE Trans. Adv. Packag.*, vol. 24, no. 4, pp. 521–527, Nov. 2001.
[4] W. Shi and J. Fang, "Evaluation of closed-form crosstalk models of coupled transmission lines," *IEEE Trans. Adv. Packag.*, vol. 22, no. 2, pp. 174–181, May 1999.
[5] C. Paul, *Introduction to Electromagnetic Compatibility*. New York: Wiley, 1992, ch. 10.
[6] C. R. Paul, *Analysis of Multiconductor Transmission Lines*. New York: Wiley, 1994.
[7] H. Shim, T. Hubing, T. Van Doren, R. DuBroff, J. Drewniak, D. Pommerenke, and R. Kaires, "Expert system algorithms for identifying radiated emission problems in printed circuit boards," in *Proc. IEEE Int. Symp. Electromagn. Compat.*, Santa Clara, CA, Aug. 9–13, 2004, vol. 1, pp. 57–62.
[8] S. Ohtsu, K. Nahase, and T. Yamagajou, "Analysis of radiation caused by LSI package cross talk and cable by using the time-domain moment method," in *Proc. IEEE Int. Symp. Electromagn. Compat.*, Minneapolis, MN, Aug. 2002, pp. 268–272.
[9] N. Oka, C. Miyazaki, and S. Nitta, "Radiation from a PCB with coupling between a low frequency and a digital signal traces," in *Proc. IEEE Int. Symp. Electromagn. Compat.*, Aug. 1998, pp. 635–640.
[10] W. Cui, M. Li, J. Drewniak, T. Hubing, T. Van Doren, R. DuBroff, and X. Luo, "Anticipating EMI from coupling between high-speed digital and I/O lines," in *Proc. IEEE Int. Symp. Electromagn. Compat.*, Seattle, WA, Aug. 1999, pp. 189–194.
[11] M. Tanaka, W. Cui, X. Luo, J. L. Drewniak, T. H. Hubing, T. P. Van Doren, and R. E. DuBroff, "FDTD modeling of EMI antennas," in *Proc. IEEE Int. Symp. Electromagn. Compat.*, 1999, pp. 560–563.
[12] W. Cui, H. Shi, X. Luo, J. L. Drewniak, T. P. Van Doren, and T. Anderson, "Lumped-element sections for modeling coupling between high-speed digital and I/O lines," in *Proc. IEEE Int. Symp. Electromagn. Compat.*, Austin, TX, Aug.1997, pp. 260–265.
[13] T. Watanabe, O. Wada, T. Miyashita, and R. Koga, "Common-mode-current generation caused by difference of unbalance of transmission lines on a printed circuit board with narrow ground pattern," *IEICE Trans. Commun.*, vol. E83-B, no. 3, pp. 593–599, Mar. 2000.
[14] T. Watanabe, H. Fujihara, O. Wada, and R. Koga, "Apreddiction method of common-mode excitation on a printed circuit board having a signal trace near the ground edge," *IEICE Trans. Commun.*, vol. E87-B, no. 8, pp. 2327–2334, Aug. 2004.
[15] Y. Toyota, T. Matsushima, K. Iokibe, R. Koga, and T. Watanabe, "Experimental validation of imbalance difference model to estimate common-mode excitation in PCBs," in *Proc. IEEE Int. Symp. Electromagn. Compat.*, Detroit, MI, Aug. 2008, pp. 1–6.
[16] T. Matsushima, T. Watanabe, Y. Toyota, R. Koga, and O. Wada, "Prediction of EMI from two-channel differential signaling system based on imbalance difference model," in *Proc. IEEE Int. Symp. Electromagn. Compat.*, Fort Lauderdale, FL, Jul. 2010, pp. 413–418.
[17] C. Su and T. Hubing, "Imbalance difference model for common-mode radiation from printed circuit boards," *IEEE Trans. Electromagn. Compat.*, vol. 53, no. 1, pp. 150–156, Feb. 2011.
[18] D. M. Pozar, *Microwave Engineering*. New York: Wiley, 2005.
[19] K. C. Gupta, R. Garg, I. Bahl, and P. Bhartia, *Microstrip Lines and Slotlines*, 2nd ed. Norwood, MA: Artech House, 1996.
[20] S. Deng, T. Hubing, and D. Beetner, "Estimating maximum radiated emissions from printed circuit boards with an attached cable," *IEEE Trans. Electromagn. Compat.*, vol. 50, no. 1, pp. 215–218, Feb. 2008.
[21] C. Su and T. Hubing, "Improvements to a method for estimating the maximum radiated emissions from PCBs with cables," *IEEE Trans. Electromagn. Compat.*, May 2011, to be published.
[22] FEKO User's Manual, Suite 6.0, EM Software & Systems, Stellenbosch, South Africa, Sep. 2010.

Changyi Su (S'08) received the B.Eng. degree from the Xian University of Technology, Xian, China, in 1993, the M.Eng. degree from Nanyang Technological University, Singapore, in 2001, and the Ph.D. degree in electrical engineering from Clemson University, Clemson, SC, in 2011.

Her research interests include electromagnetic modeling and computational electromagnetics.

Todd H. Hubing (S'82–M'82–SM'93–F'06) received the B.S.E.E. degree from the Massachusetts Institute of Technology, Cambridge, MA, in 1980, the M.S.E.E. degree from Purdue University, West Lafayette, IN, in 1982, and the Ph.D. degree in electrical engineering from North Carolina State University, Raleigh, NC, in 1988.

From 1982 to 1989, he was in the Electromagnetic Compatibility Laboratory, IBM Communications Products Division, Research Triangle Park, NC. In 1989, he became a faculty member at the University of Missouri-Rolla where he was involved with other faculty and students to analyze and develop solutions for a wide range of electromagnetic compatibility (EMC) problems affecting the electronics industry. In 2006, he joined Clemson University, Clemson, SC, as the Michelin Professor for Vehicular Electronics, where he is involved in EMC and computational electromagnetic modeling, particularly as it is applied to automotive and aerospace electronics.

Dr. Hubing is a past President of the IEEE Electromagnetic Compatibility Society and currently serves on the Society's Board of Directors. He is a Fellow of the Applied Computational Electromagnetic Society.